

# Rodinia connections between Australia and Laurentia: no SWEAT, no AUSWUS?

Michael T. D. Wingate,\* Sergei A. Pisarevsky and David A. D. Evans

*Tectonics Special Research Centre, Department of Geology and Geophysics, The University of Western Australia, 35 Stirling Highway, Crawley, WA 6009, Australia*

## ABSTRACT

Although geological comparisons between Australia and North America have provided a basis for various Neoproterozoic Rodinia reconstructions, quantitative support from precisely dated palaeomagnetic poles has so far been lacking. We report U–Pb ages and palaeomagnetic results for two suites of mafic sills within the intracratonic Bangemall Basin of Western Australia, one of which is dated at  $1070 \pm 6$  Ma and carries a high-stability palaeomagnetic remanence. Comparison of the Bangemall palaeopole with Laurentian data suggests that previous reconstructions of eastern Australia against either western Canada (SWEAT) or the western United States

(AUSWUS) are not viable at 1070 Ma. This implies that the Pacific Ocean did not form by separation of Australia–Antarctica from Laurentia, and that up to 10 000 km of late Neoproterozoic passive margins need to be matched with other continental blocks within any proposed Rodinia supercontinent. Our results permit a reconstruction (AUSMEX) that closely aligns late Mesoproterozoic orogenic belts in north-east Australia and southernmost Laurentia.

Terra Nova, 14, 121–128, 2002

## Introduction

It has been proposed that most of Earth's continental crust amalgamated during the late Mesoproterozoic (1.3–1.0 Ga) to form the supercontinent Rodinia (Hoffman, 1991). Knowledge of the configuration of the supercontinent is essential to understanding its amalgamation, and its late Neoproterozoic (0.8–0.55 Ga) breakup, which has been linked to extreme environmental and biogeochemical fluctuations and the explosive evolution of metazoan life (Valentine and Moores, 1970; Hoffman *et al.*, 1998; Karlstrom *et al.*, 2000). However, little consensus has been reached regarding the relative positions of Rodinia's constituent fragments. Most reconstructions place Australia, together with East Antarctica and India, adjacent to either western Canada (the SWEAT hypothesis, e.g. Moores, 1991; Dalziel, 1991; Hoffman, 1991; Powell *et al.*, 1993) or the western United States (the AUSWUS hypothesis; Brookfield, 1993; Karlstrom *et al.*, 1999; Burrett

and Berry, 2000). Although these models are very different (Fig. 1), each is based on matching geological and tectonic features and age provinces (so-called 'piercing points'). The available palaeomagnetic data are presently inadequate to discriminate between the SWEAT and AUSWUS alternatives. In this report we describe an integrated geochronological and palaeomagnetic study of Mesoproterozoic dolerite (diabase) sills in the western Bangemall Basin of Western Australia. The results yield a precisely dated palaeopole, BBS, at  $1070 \pm 6$  Ma, that is the most reliable of this age for Australia. We compare the BBS pole with late Mesoproterozoic poles for Laurentia and explore the implications for reconstructions between these two continents.

## Regional geology

The Mesoproterozoic Bangemall Basin (Fig. 2a) contains more than 6 km of unmetamorphosed, fine-grained carbonate and siliciclastic marine sedimentary rocks known as the Bangemall Supergroup (Muhling and Brakel, 1985; Martin *et al.*, 1999a). The basin developed on the site of the 1.83–1.78 Ga Capricorn Orogen, which formed during collision of the Pilbara and Yilgarn Cratons (Tyler and Thorne, 1990; Sheppard and Occhipinti, 2000). The Bangemall Supergroup consists of the lower Edmund Group and overlying Collier Group (Martin

*et al.*, 1999a). The Edmund Group contains ~ 4 km of stromatolitic dolomite and fine-grained clastic sediments, and unconformably overlies deformed Palaeoproterozoic rocks of the Ashburton and Bresnahan Basins in the north, and the igneous and metamorphic Gascoyne Complex in the south-west. The unconformably overlying Collier Group contains ~ 3 km of siltstone and sandstone, and, in the west, occupies a regional synclinorium that extends along the basin axis. Extensive quartz dolerite sills, classified geochemically as high-Ti continental tholeiites (Muhling and Brakel, 1985), occur throughout the Bangemall succession and are mainly concordant with bedding, although locally they transgress the stratigraphy. Sills are typically > 100 m thick, mainly medium-grained, with locally exposed chilled margins and coarse-grained phases.

The northern margin of the Bangemall Basin is relatively undeformed where it overlies the Ashburton Basin (Fig. 2a), which acted as a stable shelf during deposition. Following intrusion of dolerite sills, the southern parts of the basin were compressed northwards against the Ashburton shelf, resulting in an arcuate region of elongate, tight to open folds known as the Edmund Fold Belt (Muhling and Brakel, 1985). Folding may have been related to 1090–1060 Ma tectonothermal events (Bruguier *et al.*, 1999) in the adjacent Darling Mobile

\*Correspondence: Michael T. D. Wingate, Tectonics Special Research Centre, Department of Geology and Geophysics, The University of Western Australia, 35 Stirling Highway, Crawley, WA 6009, Australia. Tel.: +61 8 9380 2680; fax: +61 8 9380 1090; e-mail: mwingate@tsrc.uwa.edu.au

\*Details are provided in the accompanying Supplementary Material.

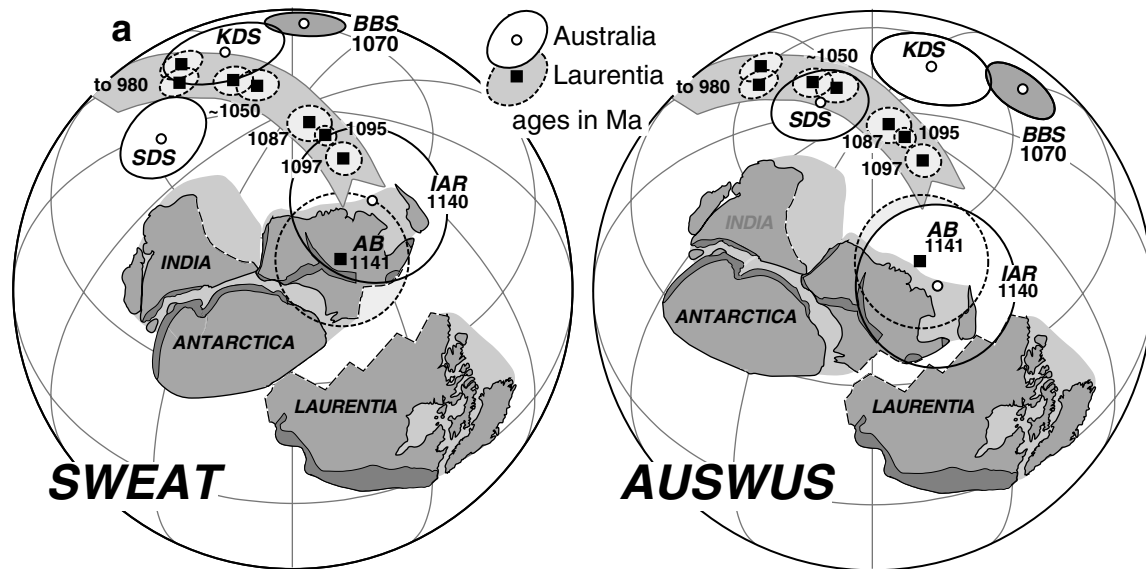


**Fig. 1** Early to mid-Neoproterozoic reconstructions of East Gondwanaland (Australia + East Antarctica + India) and Laurentia, according to (a) the SWEAT (*south-west US – East Antarctica*) and (b) AUSWUS (*Australia – western US*) hypotheses. The  $1070 \pm 6$  Ma BBS pole (shaded) obtained in this study is incompatible with Laurentian data in any reconstruction similar to SWEAT or AUSWUS. ‘Grenville-age’ mobile belts are shaded dark grey. Palaeopoles defining the Laurentian apparent polar wander (APW) path are described in the Supplementary material; also shown is the pole (AB) from the 1141 Ma Abitibi dykes (Ernst and Buchan, 1993). Australian palaeopoles include those for the 1140 Ma Lakeview dolerite, IAR (Tanaka and Idnurm, 1994; J. Claoué-Long, pers. comm., 2001), Stuart dykes, SDS (Idnurm and Giddings, 1988), and Kulgera sills, KDS (Camacho *et al.*, 1991). All palaeopoles (additional details are provided in Fig. 5 and the Supplementary material) are shown with  $\alpha_{95}$  confidence circles; arbitrary lines of longitude are  $30^\circ$  apart.

Belt (Fig. 2a), and certainly occurred prior to intrusion of N- to NE-trending dolerite dykes of the 755 Ma Mundine Well swarm (Wingate and Giddings, 2000), which are essentially undeformed and cut across all older rocks and fabrics.

### Geochronology

SHRIMP zircon ages of  $1679 \pm 6$  and  $1619 \pm 15$  Ma for underlying intrusions provide an older limit for Bangemall sedimentation (Pearson *et al.*, 1995; Nelson, 1998). SHRIMP U–Pb analyses of xenocrystic zircons from altered rhyolite near the base of the Edmund Group yielded a maximum age for eruption of  $1638 \pm 14$  Ma (Nelson, 1995). Several K–Ar and Rb–Sr studies of dolerites and baked sedimentary rocks produced ages between 1050 and 1075 Ma (Compston and Arriens, 1968; Gee *et al.*, 1976; Goode and Hall, 1981). Our SHRIMP U–Pb results\* indicate that dolerite sills were emplaced during two distinct events. For three samples (sites 1, 7 and 10; Fig. 2b), all baddeleyite and

zircon  $^{207}\text{Pb}/^{206}\text{Pb}$  ratios agree to within analytical precision and yield statistically identical ages of  $1071 \pm 8$ ,  $1067 \pm 14$  and  $1068 \pm 22$  Ma (Fig. 3). The results are combined to yield a mean age of  $1070 \pm 6$  Ma (95% confidence interval), which we regard as the time of crystallization of the younger sill suite. Zircon and baddeleyite from two sites (11 and 21) provide a mean age for the older sills of  $1465 \pm 3$  Ma.

### Palaeomagnetism

Samples were collected from dolerite sills and sedimentary rocks at 25 sites throughout the western Bangemall Basin (Fig. 2b). After removal of low-coercivity overprints by alternating field (AF) demagnetization to 10 or 20 mT, two main types of magnetic behaviour were observed. The majority of samples yielded an inconsistently directed remanence of low thermal stability (referred to as type L), which we interpret as a chemical remanent magnetization (CRM) carried mainly by maghe-

mite\*. A consistently directed magnetization (referred to as type A) was isolated in 79 samples from 15 sites (Table 1), including the three dated at *c.* 1070 Ma, and is the only stable remanence present at five sites. Unblocking temperatures between 500 °C and 580 °C show the remanence to be single component and that relatively pure magnetite is the dominant carrier (Fig. 4a). Most specimens are stable to AF treatment of 100–160 mT, and decay curves indicate variable proportions of MD and SD grains. Shale at five sites yields A magnetizations with directions similar to that of adjacent dolerite. Site mean directions converge after correction for bedding tilt, and the concentration parameter, *k*, increases from 6 to 30 (Table 1). Corrected directions are NNW with moderate downwards inclination, except at site 25, where the direction is SSE and upward (Fig. 4b). The mean direction, after tectonic correction (and inversion of data from site 25), is *D*, *I* =  $339.3^\circ$ ,  $46.5^\circ$  ( $\alpha_{95} = 8.4^\circ$ , *N* = 11 sites).

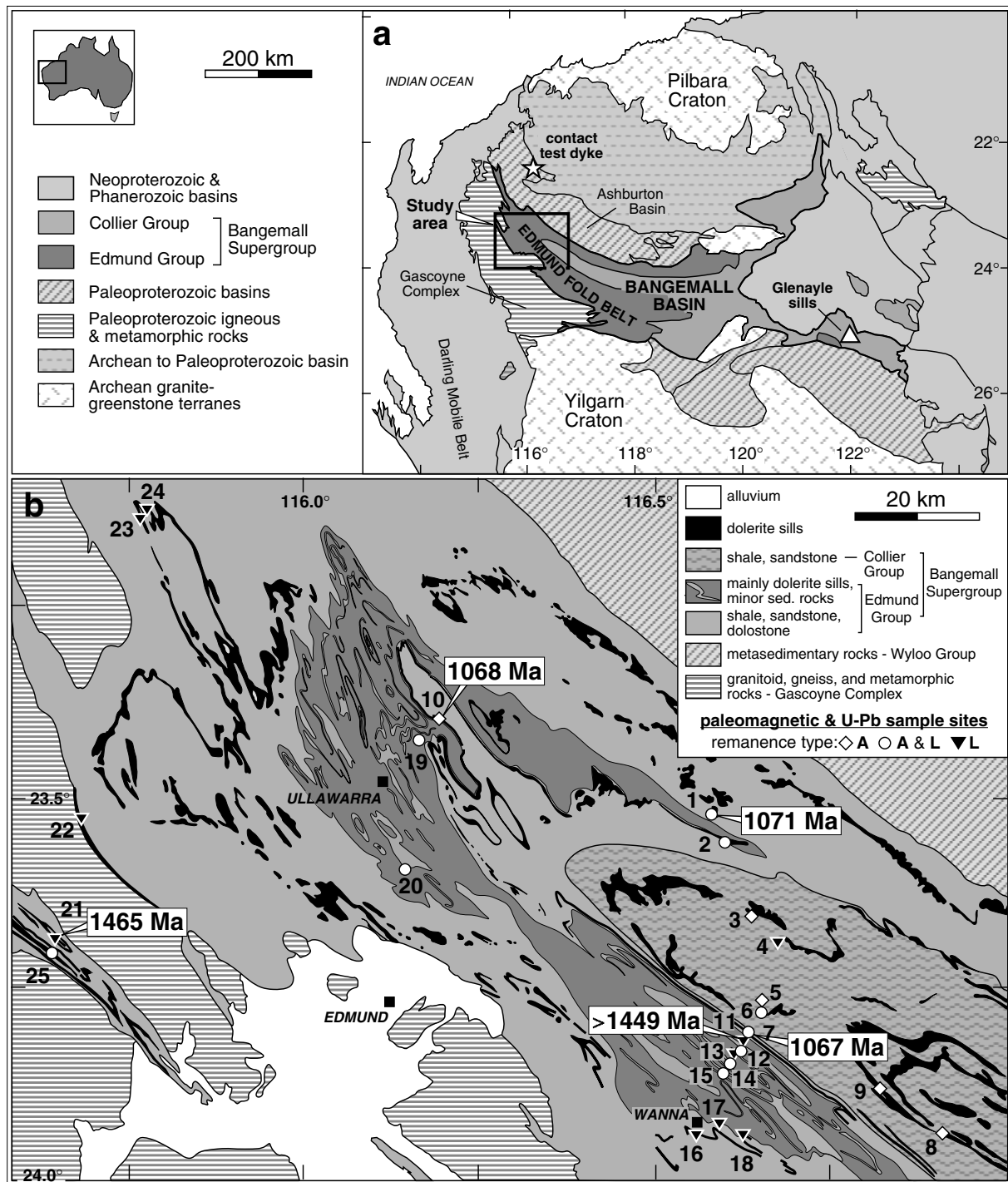


**Fig. 2** (a) Location and geological setting of the Bangemall Basin. The triangle and star indicate the location of dolerite sills in the eastern Bangemall Basin, and of a dolerite dyke, both of which yield palaeomagnetic directions similar to those obtained in this study from 1070 Ma sills. (b) Simplified geological map of the western Bangemall Supergroup (Daniels, 1969; Copp *et al.*, 1999; Martin *et al.*, 1999b), showing the locations of samples collected for palaeomagnetism and U–Pb geochronology (ages in Ma). Symbols indicate the palaeomagnetic remanence type present at each site.

Several lines of evidence indicate a primary origin for the A magnetization. (1) Low within-site dispersion is

typical of primary thermoremanent magnetizations (TRM) in rapidly cooled intrusions. (2) Positive fold

tests\* show that the A magnetization was acquired prior to folding, which may have occurred soon after sill

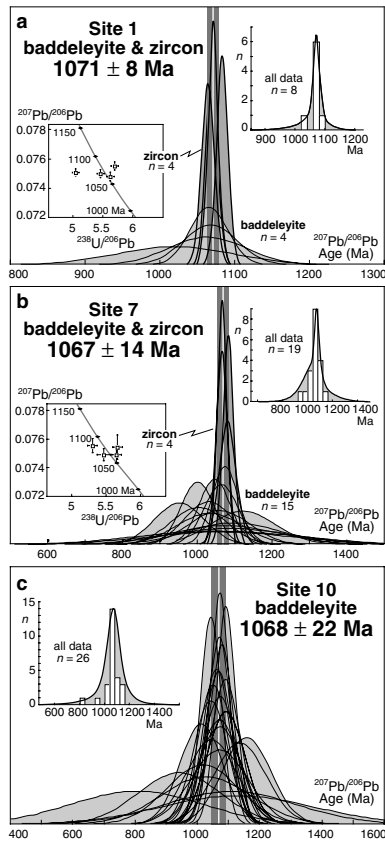


**Fig. 3** (a–c) Normalized probability density curves for individual SHRIMP  $^{207}\text{Pb}/^{206}\text{Pb}$  ages measured in baddeleyite and zircon (bold curves) from sites 1, 7 and 10. Dark grey bands indicate the weighted mean age and 95% confidence intervals. Left-hand insets in (a) and (b) show U–Pb analytical data for zircons; other insets superimpose cumulative probability density curves and histograms for all data.  $n$ , number of analyses.

intrusion at 1070 Ma. (3) Although SD magnetite grains in some sill samples require heating close to 580 °C to unblock their magnetization, previous K–Ar and Rb–Sr studies yielded ages between 1050 and 1075 Ma, and there is no evidence for a thermal event between 1070 and 755 Ma that could cause a remagnetization. (4) The presence of polarity reversals between, but not within, intrusions is supportive of a primary remanence. (5) Sedimentary rocks in baked contacts appear to be overprinted by the A magnetization. Although no stable remanence was isolated in unbaked rocks, an undated NNE-trending dyke (star, Figs 2a and 4b)

carrying the Bangemall A direction yields a positive baked-contact test\* with its host rock, the 2.45 Ga Woon-garra Rhyolite. This suggests that the dyke is similar in age to the sills (possibly comagmatic), and that the A magnetization in the sills is also original.

We conclude that the A component is a primary TRM acquired during sill emplacement at 1070 Ma. Directions of opposite polarity at site 25 imply that the intrusive event spanned at least one reversal of the Earth's magnetic field, and that, collectively, the A magnetizations adequately average palaeosecular variation. Similar palaeomagnetic directions obtained from undeformed sills in the Glenayle area\*, in the eastern Bangemall Basin (triangle, Figs 2a and 4b), together with the lack of significant deformation of the Mundine Well dyke swarm, indicate that the Bangemall Basin has undergone no internal vertical-axis rotation since 1070 Ma. The palaeomagnetic pole, BBS, lies at 33.8°N, 95.0°E ( $\alpha_{95} = 8.3^\circ$ ).

#### Comparison with previous results

Late Mesoproterozoic palaeopoles for Australia were obtained previously from the Stuart dykes and Kulgera sills in central Australia (Idnurm and Giddings, 1988; Camacho *et al.*, 1991). The Stuart dykes yielded Sm–Nd and Rb–Sr isochron ages of  $1076 \pm 33$  and  $897 \pm 9$  Ma, respectively (Black *et al.*, 1980; Zhao and McCulloch, 1993). The predominantly N-trending dolerite dykes, now locally sheared and altered, were intruded into Palaeoproterozoic basement granitoids of the southern Arunta Block, which was deformed strongly and uplifted during the Carboniferous Alice Springs orogeny (Collins and Shaw, 1995). Reliability of the preliminary SDS palaeopole is difficult to assess because no data or analytical details have been published. The shallowly S- to SE-dipping Kulgera sills yielded Sm–Nd and Rb–Sr isochron ages of  $1090 \pm 32$  and  $1054 \pm 14$  Ma, respectively (Camacho *et al.*, 1991; Zhao and McCulloch, 1993). Kulgera sills were intruded into Mesoproterozoic gneisses of the eastern Musgrave Block, which subsequently experienced late Neoproterozoic (Petermann Ranges) and Carbonifer-

ous (Alice Springs) tectonothermal events. Reliable constraints on palaeo-horizontal are not available for the Kulgera or Stuart intrusions (no tectonic corrections were applied), and both suites are located in crustal blocks that were deformed and probably re-orientated after dyke emplacement. Although isotopic data suggest that the Stuart and Kulgera intrusions are similar in age, their palaeopoles are significantly different (Fig. 1). The BBS palaeopole does not agree with the KDS or SDS poles, but is more reliable than either. The BBS pole is inferred to be primary, is dated precisely, and structural control is well-defined in adjacent sedimentary rocks. The BBS pole achieves a perfect score of  $Q = 7$  in the reliability scheme of Van der Voo (1990).

#### Implications for Rodinia reconstructions

The SWEAT reconstruction (Fig. 1a) was constrained by optimizing the fit between Australian and Laurentian poles at ~1070 and at 700–750 Ma (Powell *et al.*, 1993). However, the previous 1070 Ma poles for Australia are unreliable, as described above, and the supposedly 700–750 Ma YB dykes pole for Australia (Giddings, 1976) may represent a younger (possibly Mesozoic) overprint (Halls and Wingate, 2001). Palaeomagnetic support for the AUSWUS reconstruction (Fig. 1b) was based on matching Australian and Laurentian poles between ~1.75 and 0.75 Ga (Karlstrom *et al.*, 1999; Burrett and Berry, 2000). However, most Mesoproterozoic data for Australia are of low reliability, or are dated inadequately. A precisely dated primary pole for the Mundine Well dykes of Australia permits neither SWEAT nor AUSWUS at 755 Ma (Wingate and Giddings, 2000), although this result by itself allows either reconstruction to have been valid for earlier times. Our new BBS palaeopole permits a direct test of proposed fits at 1070 Ma, prior to any plausible age for Rodinia's fragmentation (Hoffman, 1991). Although there is no well-dated pole for Laurentia at 1070 Ma, the trend of the Laurentian APW path\* between 1100 and ~1020 Ma is well defined. The BBS pole is separated by ~30° from the Laurentian path in the SWEAT fit

**Table 1** Site mean directions and virtual geomagnetic poles (VGPs) for sites exhibiting A-type magnetization

Site	Location		Bedding		Direction ( <i>in situ</i> )				Direction (rotated)		VGP	
	Lat. (°S)	Long. (°E)	(dip/dip azimuth)	<i>n</i>	<i>D</i> (°)	<i>I</i> (°)	<i>k</i>	$\alpha_{95}$ (°)	<i>D'</i> (°)	<i>I'</i> (°)	Lat. (°N)	Long. (°E)
1	23.522	116.580	13/088	9(3)	344.9	48.4	75	5.6	359.8	48.7	<b>36.8</b>	116.4
2*	23.557	116.597	35/213	(2)	017.6	22.3	151	14.4	007.4	54.9	30.6	123.6
3	23.653	116.633	04/353	5	336.4	37.7	108	6.6	337.2	33.9	42.3	86.9
5	23.765	116.650	01/134	(5)	328.5	50.5	610	2.8	328.5	51.5	26.5	87.0
6	23.783	116.652	02/320	8(3)	337.4	37.1	41	8.2	337.0	35.2	41.3	87.3
7	23.807	116.630	60/041	6(2)	267.9	49.3	37	10.1	352.4	50.6	34.4	108.8
8	23.938	116.910	29/029	6	312.1	57.7	257	3.8	343.7	42.9	38.7	97.9
9	23.875	116.820	19/233	6	344.7	40.9	97	6.2	327.2	45.2	30.3	82.7
10	23.401	116.192	43/028	6	268.1	65.3	575	2.6	350.2	53.8	31.5	106.7
12	23.822	116.626	80/034	5	244.8	22.6	195	4.9	331.0	58.0	21.9	92.6
14*	23.838	116.613	43/072	2	324.1	52.3	1436	4.7	016.6	45.0	37.1	135.3
15	23.855	116.606	74/205	4	002.8	5.1	20	18.1	319.9	65.2	10.1	90.2
19*	23.426	116.172	07/178	2	346.3	47.0	151	14.4	344.8	53.3	30.9	101.5
20*	23.589	116.145	65/055	2	268.6	46.5	183	13.1	012.5	55.7	29.0	127.7
25	23.708	115.633	79/038	11	111.3	−37.5	40	6.9	164.1	−19.9	52.6	89.3
dyke	22.197	116.290	–	9	341.9	60.0	159	4.1	–	–	24.7	101.3
Mean direction ( <i>in situ</i> ):				11 sites	316.7	47.9	6	19.8	Palaeopole:		33.8	95.0
Mean direction (rotated):				11 sites	339.9	46.5	30	8.4	<i>n</i> = 11 sites, <i>K</i> = 32, <i>A</i> <sub>95</sub> = 8.3°			

Results from four sites (marked with asterisks) that each yielded two data points, although consistent with the remaining data, are considered less reliable and were not included in calculating mean results. Results listed for the dyke (including its baked contact) were also not included in calculations. *n*, number of samples given unit weight in calculation of mean (number of sedimentary rock samples included in parentheses); *D*, declination (E of N); *I*, inclination (positive downwards); *k* (*K*), Fisher's precision parameter;  $\alpha_{95}$ , (*A*<sub>95</sub>), circle of 95% confidence about mean direction (pole). VGPs are calculated from rotated (bedding-corrected) directions.

and by at least 40° in the AUSWUS fit (Fig. 1). Moreover, a fit similar to SWEAT or AUSWUS cannot be achieved by matching the BBS pole with any part of the Laurentian path shown in Fig. 1, indicating that neither reconstruction is viable at 1070 Ma.

To explore possible reconstructions between Australia and Laurentia, we approximate a pole position for Laurentia at 1070 Ma by assuming constant APW between the 1087 and ~1050 Ma poles. Superimposing the BBS palaeopole and this interpolated pole position for Laurentia at the projection axis (Fig. 5) places the continents at their correct orientations and palaeolatitudes at 1070 Ma. Australia is situated at lower palaeolatitudes than is permitted by the SWEAT or AUSWUS models, placing the Cape River Province of north-east Australia at a similar latitude to the south-west end of the ~1250–980 Ma Grenville Province of Laurentia (Rivers, 1997). High-grade metamorphic and magmatic rocks in the Cape River Province contain 1240, 1145 and 1105 Ma zircon age components, and may correlate with 'Grenville-age' rocks in the Musgrave and

Albany–Fraser orogens (Blewett *et al.*, 1998). The Grenville Province may therefore have continued through Australia. The time at which Australia and Laurentia might have come together is unknown, but can be investigated by comparing older palaeopoles from each block. The tight reconstruction in Fig. 5 permits the  $\alpha_{95}$  confidence circles of the 1140 Ma IAR and AB poles to overlap, although these two poles are insufficiently precise for a rigorous test.

Owing to the lack of palaeolongitude control, it is entirely possible that Australia and Laurentia were not joined at 1070 Ma. In addition, because final 'Grenvillian' assembly of Rodinia could conceivably post-date 1070 Ma, there remains the possibility that fits similar to SWEAT or AUSWUS could have been achieved through a post-1070 Ma collision between a unified Australian–Mawson craton and some part of the proto-Cordilleran Laurentian margin. In this case an intermediary craton would appear to be required to bear the main record of such a collision (e.g. South China; Li *et al.*, 2001), evidence for which is largely lacking

in eastern Australia and western North America. Moreover, similarities among Palaeoproterozoic and early Mesoproterozoic rocks in Australia and North America would be fortuitous, removing some of the very foundations for the SWEAT and AUSWUS models.

The provocative fit suggested in Fig. 5, referred to here as AUSMEX (Australia – Mexico), requires further testing by comparing additional Proterozoic palaeopoles of precisely the same age from Australia and Laurentia, with subsequent reconstructions to be elaborated using geological and other constraints. The most compelling geological arguments used to generate the SWEAT and AUSWUS hypotheses, including correlation of Mesoproterozoic orogenic belts, Palaeo- and Mesoproterozoic isotopic age provinces, and Neoproterozoic rift – passive margin sedimentary successions, remain robust in the AUSMEX reconstruction. The SWEAT and AUSWUS models implied that Neoproterozoic separation of Australia–Antarctica from Laurentia led to opening of the Pacific Ocean. The results of this study, however, suggest

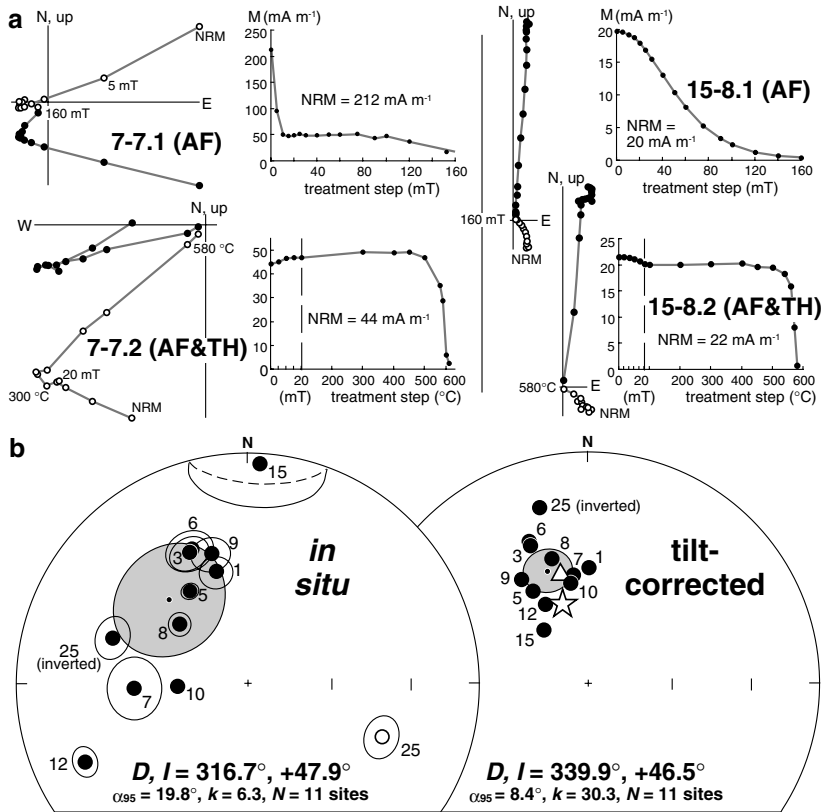


**Fig. 4** (a) Examples of alternating field (AF) and thermal (TH) demagnetization of A-type remanence in two specimens of a single core from each of sites 7 and 15. Orthogonal projections show trajectories of vector endpoints during progressive demagnetization (open/closed symbols represent vertical/horizontal plane). Demagnetization curves show changes in intensity during treatment. Reference frame is present horizontal. (b) Component A site mean directions in geographical (*in situ*) and stratigraphic (tilt-corrected) coordinates. Open/closed symbols in lower-hemisphere equal-angle stereographic projections indicate upward/downward pointing directions. The overall mean direction in each case is shown with a shaded  $\alpha_{95}$  circle. The mean direction for site 25 was inverted through the origin prior to statistical calculations. The star and triangle show mean palaeomagnetic directions obtained for a NNE-trending dyke that yields a positive baked-contact test, and for nine sites in undeformed dolerite sills in the eastern Bangemall Basin, respectively (described in the Supplementary material). *D*, declination (E of N); *I*, inclination (positive downwards);  $\alpha_{95}$ , semi-angle of cone of 95% confidence about mean direction; *k*, Fisher's precision parameter.

that western Laurentia was not the conjugate margin to eastern Australia–Antarctica. The origin of the Pacific Ocean is therefore undetermined, and up to 10 000 km of late Neoproterozoic passive margins in eastern Australia and western Laurentia need to be matched with other continental blocks within any proposed Rodinia supercontinent.

### Supplementary material

The following material is available from <http://blackwell-science.com/>

products/journals/suppmat/TER/TER401/TER401sm.html

**Table S1** Ion microprobe data for baddeleyite and zircon from site 1.

**Table S2** Ion microprobe analytical data for baddeleyite and zircon from site 7.

**Table S3** Ion microprobe data for baddeleyite from site 10.

**Table S4** Selected late Mesoproterozoic palaeopoles for Laurentia.

**Fig. S1** Examples of AF and thermal demagnetization of L-type remanence in two specimens of a single core from each of sites 15 (a) and 25 (b).

Orthogonal projections show trajectories of vector endpoints during progressive demagnetization (open/closed symbols represent vertical/horizontal plane). Open/closed symbols in lower-hemisphere equal-area stereographic projections indicate upward/downward pointing directions. Reference frame is present horizontal. Demagnetization curves show changes in magnetization intensity during treatment.

**Fig. S2.** Directions and thermal demagnetization for A- and L-type magnetizations at site 15 (a) and L-type magnetizations at site 21 (b). Demagnetization curves are normalized to values at 100 °C. The mean direction and  $\alpha_{95}$  confidence circle are shown for four A-type directions at site 15. Other notes as in Fig. S1.

**Fig. S3.** (a) Outcrop sketch for the baked-contact test between a dolerite dyke and Woongarra Rhyolite. (b) Palaeomagnetic directions;  $\alpha_{95}$  confidence circles are shown around the mean for each group. (c) Examples of thermal demagnetization of four specimens (distance from dyke contact shown in parentheses). Other notes as in Fig. S1.

### Acknowledgments

This research was supported by Australian Postdoctoral Research Fellowships (M.W. and D.E.) from the Australian Research Council, funding and logistical support from the Geological Survey of Western Australia (M.W.) and the Tectonics Special Research Centre. The assistance and advice of David Martin, David Nelson, Franco Pirajno, and Alan Thorne are gratefully appreciated. Nien Schwarz assisted with field sampling. Palaeomagnetic analyses were carried out at the Black Mountain laboratory, Canberra, a joint facility of the Australian Geological Survey Organization and the Australian National University, and at the Department of Geology and Geophysics at the University of Western Australia. U–Pb measurements were conducted using the Perth SHRIMP II ion microprobe, operated by a consortium consisting of the Geological Survey of Western Australia, the University of Western Australia, and Curtin University of Technology, with the support of the Australian Research Council. David Nelson assisted with SHRIMP measurements. Reconstructions were explored using Plates software from the University of Texas at Austin. Thanks to Ian Dalziel, Paul Hoffman, Joe Meert, Brendan Murphy, and

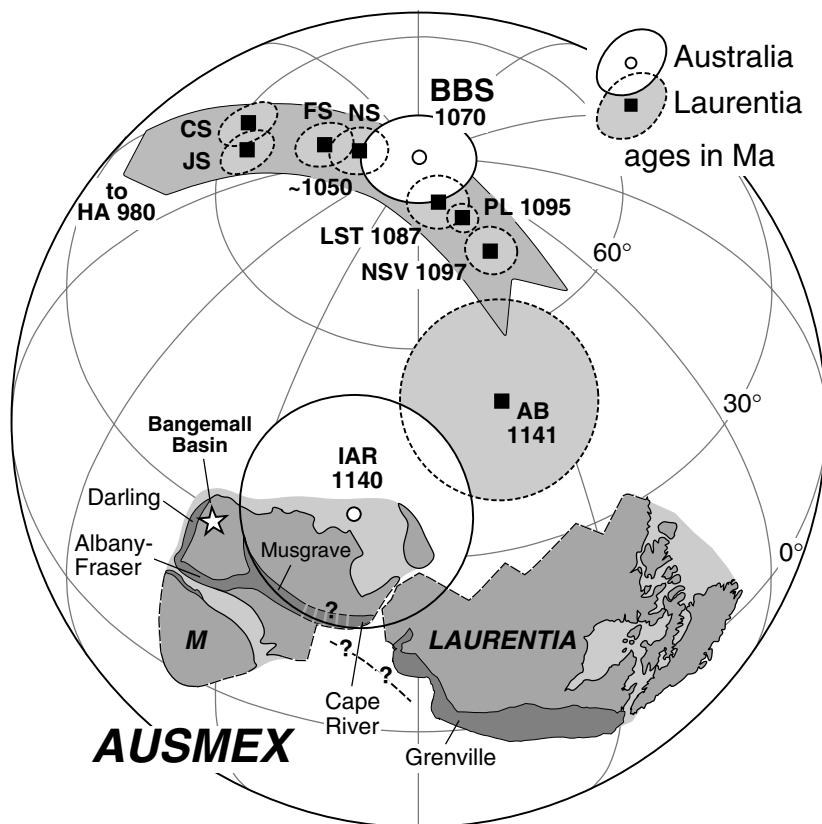


**Fig. 5** A possible reconstruction (AUSMEX) between Australia and Laurentia at 1070 Ma that places the Grenville and Cape River provinces at similar palaeolatitudes. Note that palaeolongitudes are not constrained when comparing individual pole positions. M is the Mawson block of East Antarctica according to Fitzsimons (2000). Orogenic belts discussed in the text are labelled. Rotation parameters (clockwise positive): Australia to absolute frame, 41.49°N, 34.51°E, 79.53°; Laurentia to Australia, 54.52°N, 149.86°E, – 120.80°. Other notes as in Fig. 1.

Trond Torsvik for constructive comments. This is Tectonics Special Research Centre publication number 168, and a contribution to International Geological Correlation Program (IGCP) Project 440.

## References

- Black, L.P., Shaw, R.D. and Offe, L.A., 1980. The age of the Stuart dyke swarm and its bearing on the onset of Late Precambrian sedimentation in central Australia. *J. Geol. Soc. Aust.*, **27**, 151–155.
- Blewett, R.S., Black, L.P., Sun, S.S., Knutson, J., Hutton, L.J. and Bain, J.H.C., 1998. U-Pb zircon and Sm-Nd geochronology of the Mesoproterozoic of North Queensland: implications for a Rodinian connection with the belt Supergroup of North America. *Precamb. Res.*, **89**, 101–127.
- Brookfield, M.E., 1993. Neoproterozoic Laurentia-Australia fit. *Geology*, **21**, 683–686.
- Bruguier, O., Bosch, D., Pidgeon, R.T., Byrne, D.I. and Harris, L.B., 1999. U-Pb chronology of the Northampton Complex, Western Australia – evidence for Grenvillian metamorphism, sedimentation, and deformation and geodynamic implications. *Contrib. Mineral. Petrol.*, **136**, 258–272.
- Burrett, C. and Berry, R., 2000. Proterozoic Australia – Western United States (AUSWUS) fit between Laurentia and Australia. *Geology*, **28**, 103–106.
- Camacho, A., Simons, B. and Schmidt, P.W., 1991. Geological and paleomagnetic significance of the Kulgera Dyke Swarm, N.T., Australia. *Geophys. J. Int.*, **107**, 37–45.
- Collins, W.J. and Shaw, R.D., 1995. Geochronological constraints on orogenic events in the Arunta Inlier: a review. *Precamb. Res.*, **71**, 315–346.
- Compston, W. and Arriens, P.A., 1968. The Precambrian geochronology of Australia. *Can. J. Earth Sci.*, **5**, 561–583.
- Copp, I.A., Martin, D.McB., Thorne, A.M. and Bagas, L., 1999. Ullawarra, W.A., Sheet. 2151. *W. Aust. Geol. Surv., 1: 100 000 Geol. Series*. Geological Survey of Western Australia, Perth.
- Dalziel, I.W.D., 1991. Pacific margins of Laurentia and East Antarctica-Australia as a conjugate rift pair: Evidence and implications for an Eocambrian supercontinent. *Geology*, **19**, 598–601.
- Daniels, J.L., 1969. Edmund, W.A. *W. Aust. Geol. Surv., 1: 250 000 Geol. Series*. Geological Survey of Western Australia, Perth.
- Ernst, R.E. and Buchan, K.L., 1993. Paleomagnetism of the Abitibi dike swarm, southern Superior Province, and implications for the Logan Loop. *Can. J. Earth Sci.*, **30**, 1886–1897.
- Fitzsimons, I.C.W., 2000. Grenville-age basement provinces in East Antarctica: Evidence for three separate collisional orogens. *Geology*, **28**, 879–882.
- Gee, R.D., De Laeter, J.R. and Drake, J.R., 1976. Geology and geochronology of altered rhyolite from the lower part of the Bangemall Group near Tangadee, Western Australia. *W. Aust. Geol. Surv. Ann. Report*, **1975**, 112–117.
- Giddings, J.W., 1976. Precambrian paleomagnetism in Australia I: basic dykes and volcanics from the Yilgarn Block. *Tectonophysics*, **30**, 91–108.
- Goode, A.D.T. and Hall, W.D.M., 1981. The middle Proterozoic eastern Bangemall Basin, Western Australia. *Precamb. Res.*, **16**, 11–29.
- Halls, H.C. and Wingate, M.T.D., 2001. Paleomagnetic pole from the Yilgarn B (YB) dykes of Western Australia: no longer relevant to Rodinia reconstructions. *Earth Planet. Sci. Lett.*, **187**, 39–53.
- Hoffman, P.F., 1991. Did the breakout of Laurentia turn Gondwanaland inside-out? *Science*, **252**, 1409–1412.
- Hoffman, P.F., Kaufman, A.J., Halverson, G.P. and Schrag, D.P., 1998. A Neoproterozoic Snowball Earth. *Science*, **281**, 1342–1346.
- Idnurm, M. and Giddings, J.W., 1988. Australian Precambrian polar wander: a review. *Precamb. Res.*, **40**, 61–88.
- Karlstrom, K.E., Bowring, S.A., Dehler, C.M., Knoll, A.H., Porter, S.M., Des Marais, D.J., Weil, A.B., Sharp, Z.D., Geissman, J.W., Elrick, M.B., Timmons, J.M., Crossey, L.J. and Davidek, K.L., 2000. Chuar Group of the Grand Canyon: Record of breakup of Rodinia, associated change in the global carbon cycle, and ecosystem expansion by 740 Ma. *Geology*, **28**, 619–622.
- Karlstrom, K.E., Harlan, S.S., Williams, M.L., McLelland, J. and Geissman, J.W., 1999. Refining Rodinia: geologic evidence for the Australia–Western U.S.

- connection in the Proterozoic. *GSA Today*, **9**, 1–7.
- Li, Z.X., Li, X.H., Zhou, H. and Kinny, P.D., 2001. Grenville-age continental collision in South China: New SHRIMP age constraints and implications to Rodinia configuration. *Geol. Soc. Aust. Abstract.*, **65**, 78–79.
- Martin, D.McB., Thorne, A.M. and Copp, I.A., 1999a. A provisional revised stratigraphy for the Bangemall Group on the Edmund 1: 250 000 sheet. *W. Aust. Geol. Surv. Ann. Rev.*, **1998–99**, 51–55.
- Martin, D.McB., Thorne, A.M. and Copp, I.A., 1999b. Elliot Creek, W.A. Sheet 2250. *W. Aust. Geol. Surv., 1: 100 000 Geological Series*. Geological Survey of Western Australia, Perth.
- Moore, E.M., 1991. Southwest U.S.–East Antarctic (SWEAT) connection: a hypothesis. *Geology*, **19**, 425–428.
- Muhling, P.C. and Brakel, A.T., 1985. Geology of the Bangemall Group – the evolution of an intracratonic Proterozoic basin. *W. Aust. Geol. Surv. Bull.*, **128**, 266pp.
- Nelson, D.R., 1995. Compilation of SHRIMP U-Pb zircon geochronological data, 1994. *W. Aust. Geol. Surv. Rec.*, **1995/3**, 244pp.
- Nelson, D.R., 1998. Compilation of SHRIMP U-Pb zircon geochronological data, 1997. *W. Aust. Geol. Surv. Rec.*, **1998/2**, 242pp.
- Pearson, J.M., Taylor, W.R. and Barley, M.E., 1995. Geology of the alkaline Gifford Creek Complex, Gascoyne Province, Western Australia. *Aust. J. Earth Sci.*, **43**, 299–309.
- Powell, C.McA., Li, Z.X., McElhinny, M.W. et al., 1993. Paleomagnetic constraints on timing of the Neoproterozoic breakup of Rodinia and the Cambrian formation of Gondwana. *Geology*, **21**, 889–892.
- Rivers, T., 1997. Lithotectonic elements of the Grenville province: review and tectonic implications. *Precamb. Res.*, **86**, 117–154.
- Sheppard, S. and Occhipinti, S.A., 2000. Errabiddy and Landor 1: 100 000 sheets. *W. Aust. Geol. Surv., Explan. Notes*, 26p. Geological Survey of Western Australia, Perth.
- Tanaka, H. and Idnurm, M., 1994. Paleomagnetism of Proterozoic mafic intrusions and host rocks of the Mt. Isa Inlier, Australia. *Precamb. Res.*, **69**, 241–258.
- Tyler, I.M. and Thorne, A.M., 1990. The northern margin of the Capricorn Orogen, Western Australia – an example of an early Proterozoic collision zone. *J. Struct. Geol.*, **12**, 685–701.
- Valentine, J.W. and Moores, E.M., 1970. Plate-tectonic regulation of faunal diversity and sea level: a model. *Nature*, **228**, 657–659.
- Van der Voo, R., 1990. The reliability of paleomagnetic data. *Tectonophysics*, **184**, 1–9.
- Wingate, M.T.D. and Giddings, J.W., 2000. Age and paleomagnetism of the Mundine Well dyke swarm, Western Australia: implications for an Australia–Laurentia connection at 755 Ma. *Precamb. Res.*, **100**, 335–357.
- Zhao, J.-X. and McCulloch, M.T., 1993. Sm-Nd mineral isochron ages of Late Proterozoic dyke swarms in Australia: evidence for two distinct events of mafic magmatism and crustal extension. *Chem. Geol.*, **109**, 341–354.

Received 31 July 2001; revised version accepted 17 January 2002

## ***A revised Rodinia supercontinent: no SWEAT, no AUSWUS***

**Michael T.D. Wingate, Sergei A. Pisarevsky, and David A.D. Evans**

---

### **1. Project strategy**

The Bangemall sills were targeted as part of our on-going programme of integrated paleomagnetism and U-Pb geochronology of mafic intrusive rocks in Australia, aimed at improving the Proterozoic apparent polar wander (APW) path for Australia and at testing Proterozoic supercontinent reconstructions. Previous Rb-Sr and K-Ar geochronology suggests that the sills were emplaced at about 1050 to 1075 Ma and so might be useful in testing Rodinia hypotheses. Mafic sills and dykes tend to be excellent recorders of the Earth's magnetic field, and because they cool quickly, their crystallisation age, as determined accurately and precisely by U-Pb methods on zircon and baddeleyite, can be taken as the age of primary magnetisation. Both zircon and baddeleyite are relatively common in the coarse-grained differentiated portions of many mafic intrusions, and late-stage zircons tend to be highly enriched in uranium (and therefore radiogenic Pb) and yield precise isotopic ratios. The sedimentary rocks into which the Bangemall sills are intruded provide excellent structural control, and local folding permits the application of fold tests to establish remanence stability. In addition, the Bangemall sills outcrop over several hundred kilometres (Fig. 2a), enabling possible post-magnetisation tectonic rotations to be assessed by comparing magnetisation directions from widely-separated parts of the basin.

### **2. SHRIMP U-Pb Geochronology**

#### **Analytical details**

Samples of coarse-grained dolerite were collected from sites 1, 7, 10, 11, and 21. For each sample, about 500 g of rock was processed by conventional magnetic and density techniques to concentrate non-magnetic, heavy fractions. Baddeleyite and zircon crystals were extracted from concentrates by hand-picking under a binocular microscope. Both zircon and baddeleyite were recovered from sites 1 and 7, and 21, whereas only baddeleyite was obtained from site 10, and only zircon from site 11. For zircon, U-Th-Pb ratios and absolute abundances were determined relative to the CZ3 standard zircon ( $^{206}\text{Pb}/^{238}\text{U} = 0.09143$  (564 Ma), 550 ppm  $^{238}\text{U}$ ; Nelson, 1997), analyses of which were interspersed with those of unknown grains, using operating and data processing procedures similar to those described by Compston *et al.* (1992) and Nelson (1997). Ratios of  $^{206}\text{Pb}/^{238}\text{U}$  measured in baddeleyite by ion microprobe have been shown to vary significantly and systematically with the relative orientation of the baddeleyite crystal structure and the direction of the primary ion beam, therefore baddeleyite ages are based only on  $^{207}\text{Pb}/^{206}\text{Pb}$  ratios, which are unaffected by this phenomenon (Wingate and Compston, 2000). Calculated  $^{238}\text{U}$  and  $^{232}\text{Th}$  concentrations for baddeleyite are

approximate, owing mainly to heterogeneity in  $^{238}\text{U}$  in the Phalaborwa baddeleyite (for which a value of 300 ppm  $^{238}\text{U}$  was assumed), but are proportional to true values within each analytical session. For both zircon and baddeleyite, measured compositions were corrected for common Pb using non-radiogenic  $^{204}\text{Pb}$  and an average crustal composition (Cumming and Richards, 1975) appropriate to the age of the mineral. Decay constants employed are those recommended by Steiger and Jäger (1977).

## Results

**Site 1:** About 50 zircons and 20 baddeleyite crystals were recovered. Most baddeleyites are fragments of larger euhedral crystals, and only four were of sufficient size to analyse by SHRIMP. Four analyses of three zircons and four analyses of four baddeleyites were obtained (Table A1). Zircon  $^{207}\text{Pb}/^{206}\text{Pb}$  ratios agree to within analytical precision, yielding a mean age of  $1071.5 \pm 3.6$  ( $1\sigma$ ). Corresponding  $^{238}\text{U}/^{206}\text{Pb}$  ratios are dispersed beyond analytical precision; the reversely discordant analysis (Z8.1) yields an age of 1166 Ma and possesses the highest U and Th content. Ratios of  $^{207}\text{Pb}/^{206}\text{Pb}$  for 4 baddeleyite analyses agree to within uncertainty, yielding a mean age of  $1062.9 \pm 18.6$  Ma. All baddeleyite and zircon  $^{207}\text{Pb}/^{206}\text{Pb}$  ratios agree to within analytical precision (Fig. 3a) and yield an age of  $1071 \pm 8$  Ma (95% confidence interval), interpreted as the age of crystallisation of the sill.

**Site 7:** Four zircons and 34 baddeleyite crystals were recovered. Fifteen analyses were conducted of 15 baddeleyites (Table A2). Ratios of  $^{207}\text{Pb}/^{206}\text{Pb}$  from two analytical sessions agree to within large uncertainties, yielding mean ages of  $1040.3 \pm 18.5$  Ma ( $n = 10$ ) for session 1 and  $1050.1 \pm 45.4$  Ma ( $n = 5$ ) for session 2 (both  $\pm 1\sigma$ ). Low precision reflects the very low content of radiogenic Pb in these baddeleyites, and hence the large relative contribution to final uncertainties from common Pb correction. Of four zircons recovered, two crystals (Z2, Z3) yielded  $^{207}\text{Pb}/^{206}\text{Pb}$  ages of 2156 and 1798 Ma, respectively, and are considered to be xenocrysts. Zircons Z1 (3 analyses) and Z4 (1 analysis) are highly enriched in  $^{238}\text{U}$  and  $^{232}\text{Th}$ , contain negligible common Pb, and yield a mean  $^{207}\text{Pb}/^{206}\text{Pb}$  age of  $1072 \pm 7$  Ma ( $1\sigma$ ). Excluding data from the two xenocrysts, all baddeleyite and zircon  $^{207}\text{Pb}/^{206}\text{Pb}$  ratios (Fig. 3b) agree to within analytical precision and yield an age of  $1067 \pm 14$  Ma (95% confidence interval), interpreted as the crystallisation age of the sill.

**Site 10:** About fifty baddeleyite crystals and crystal fragments, but no zircons, were separated from this sample. Twenty-six analyses were conducted on 19 baddeleyite crystals (Table A3). Large uncertainties for four analyses reflect low uranium content (and hence low radiogenic Pb) as well as relatively large corrections for common Pb. All ratios of  $^{207}\text{Pb}/^{206}\text{Pb}$  agree to within analytical precision (Fig. 3c), yielding a weighted mean age of  $1068 \pm 22$  Ma (95% confidence interval), interpreted as the crystallisation age of the sill.

**Older sills:** Analyses of high U and Th zircons from sites 11 and 21 exhibit reverse discordance correlated with increasing U and Th concentration. This phenomenon (observed also in zircons from sites 1 and 7, above), is common in ion microprobe analyses of variably metamict zircons that are highly enriched in U and Th, and is believed to reflect enhanced sputtering of Pb relative to U due to

radiation-induced microstructural changes (McLaren et al., 1994). Zircons from site 11 show evidence for reverse discordance superimposed with ancient Pb loss. The eight oldest  $^{207}\text{Pb}/^{206}\text{Pb}$  ratios yield a minimum age of  $1449 \pm 5$  Ma. Zircon and baddeleyite from site 21 furnish a mean  $^{207}\text{Pb}/^{206}\text{Pb}$  age of  $1465 \pm 3$  Ma, which is regarded as the time of emplacement of the older sill suite. Because no useful paleomagnetic data were obtained from the older sills, the geochronology of sites 11 and 21 will be discussed in more detail elsewhere.

### Ion microprobe analytical data

Tables A1 to A3 contain U-Pb analytical data for baddeleyite and zircon samples from sites 1, 7, and 10. Analyses are listed in the order in which they were conducted.  $f_{206}$  is the proportion of common  $^{206}\text{Pb}$  in total measured  $^{206}\text{Pb}$ . Pb\* indicates radiogenic Pb. Uncertainties for zircon  $^{206}\text{Pb}/^{238}\text{U}$  ratios do not include a component arising from calibration against the CZ3 zircon standard. Within a single analytical session, relative  $^{206}\text{Pb}/^{238}\text{U}$  ages of individual analyses are assessed correctly using their observed uncertainties, without calibration error included. When the uncertainty of an "absolute"  $^{206}\text{Pb}/^{238}\text{U}$  age is reported for the mean of a group, it is necessary to add, in quadrature, the uncertainty (coefficient of variation) in the mean  $^{206}\text{Pb}/^{238}\text{U}$  determined for the CZ3 standard. The calibration uncertainty ( $1\sigma$ ) is provided below for each zircon session.

**Table A1** Ion microprobe data for baddeleyite and zircon from site 1.

Grain Area	$^{238}\text{U}$ (ppm)	$^{232}\text{Th}$ (ppm)	Th/U	$f_{206}$ (%)	$^{206}\text{Pb}^*/^{238}\text{U}$ ( $\pm 1\sigma$ )		$^{207}\text{Pb}^*/^{206}\text{Pb}^*$ ( $\pm 1\sigma$ )		$^{207}\text{Pb}^*/^{206}\text{Pb}^*$ age (Ma)	( $\pm 1\sigma$ )
<i>Baddeleyite</i>										
1.1	425	442	1.04	0.133	---	---	0.07488	0.00093	1065	25
2.1	140	33	0.23	0.660	---	---	0.07481	0.00194	1063	52
3.1	179	29	0.16	0.193	---	---	0.07495	0.00132	1067	36
4.1	134	7	0.06	0.994	---	---	0.07321	0.00284	1020	79
<i>Zircon</i>										
Z6.1	1164	4927	4.2	0.021	0.1756	0.0019	0.07553	0.00028	1083	7
Z6.2	1245	5132	4.1	0.071	0.1778	0.0020	0.07482	0.00030	1064	8
Z7.1	1238	3628	2.9	0.067	0.1832	0.0020	0.07500	0.00027	1069	7
Z8.1	1897	8839	4.7	0.064	0.1983	0.0022	0.07508	0.00024	1071	6

Zircon  $^{206}\text{Pb}/^{238}\text{U}$  calibration uncertainty: 1.14%

**Table A2** Ion microprobe analytical data for baddeleyite and zircon from site 7.

Grain Area	$^{238}\text{U}$ (ppm)	$^{232}\text{Th}$ (ppm)	Th/U	$f_{206}$ (%)	$^{206}\text{Pb}^*/^{238}\text{U}$ ( $\pm 1\sigma$ )		$^{207}\text{Pb}^*/^{206}\text{Pb}^*$ ( $\pm 1\sigma$ )		$^{207}\text{Pb}^*/^{206}\text{Pb}^*$ age (Ma)	( $\pm 1\sigma$ )
<i>Baddeleyite</i>										
1.1	33	5	0.16	0.567	---	---	0.07079	0.00236	951	67
2.1	47	7	0.15	0.373	---	---	0.07250	0.00160	1000	44
3.1	20	2	0.12	0.037	---	---	0.07698	0.00341	1121	86
4.1	19	2	0.10	1.210	---	---	0.07574	0.00676	1088	169
5.1	78	28	0.36	0.204	---	---	0.07517	0.00134	1073	36

6.1	31	5	0.17	5.990	---	---	0.07536	0.00852	1078	212
7.1	36	7	0.19	0.126	---	---	0.07481	0.00175	1063	46
8.1	39	6	0.15	0.396	---	---	0.07368	0.00332	1033	88
9.1	20	1	0.02	0.409	---	---	0.07261	0.00274	1003	75
10.1	40	3	0.06	0.145	---	---	0.07414	0.00159	1045	43
11.1	69	13	0.19	0.318	---	---	0.07358	0.00240	1030	64
12.1	28	3	0.11	1.024	---	---	0.07612	0.00501	1098	126
13.1	24	3	0.13	0.667	---	---	0.07521	0.00563	1074	144
14.1	20	1	0.05	1.663	---	---	0.07400	0.00816	1042	208
15.1	38	6	0.17	0.435	---	---	0.07464	0.00309	1059	81
<i>Zircon, session 1</i>										
Z1.1	2582	8817	3.4	0.014	0.1765	0.0021	0.07544	0.00086	1080	23
<sup>†</sup> Z2.1	273	117	0.4	0.066	0.3402	0.0039	0.13438	0.00095	2156	12
<i>Zircon, session 2</i>										
Z1.2	2112	6793	3.2	0.007	0.1886	0.0025	0.07553	0.00051	1083	13
Z1.3	2820	14544	5.2	0.039	0.1829	0.0032	0.07491	0.00043	1066	11
<sup>†</sup> Z3.1	1636	525	0.3	0.933	0.3106	0.0033	0.10989	0.00118	1798	19
Z4.1	2529	12651	5.0	0.040	0.1770	0.0022	0.07488	0.00054	1065	14

<sup>†</sup> xenocrystic zircon; zircon <sup>206</sup>Pb/<sup>238</sup>U calibration uncertainty (*session 1*): 0.96%; (*session 2*): 1.27%

**Table A3** Ion microprobe analytical data for baddeleyite from site 10.

Grain	<sup>238</sup> U	<sup>232</sup> Th	Th/U	<i>f</i> <sub>206</sub>	<sup>207</sup> Pb*/ <sup>206</sup> Pb*		<sup>207</sup> Pb*/ <sup>206</sup> Pb* age	
Area	(ppm)	(ppm)		(%)	(±1σ)		(Ma)	(±1σ)
1.1	95	52	0.55	1.032	0.07046	0.00475	942	132
2.1	58	15	0.26	5.218	0.07724	0.01030	1127	246
3.1	107	8	0.08	0.248	0.07471	0.00165	1061	44
4.1	119	13	0.11	0.637	0.07412	0.00305	1045	81
5.1	38	2	0.06	1.408	0.06596	0.00712	805	211
6.1	199	28	0.14	0.133	0.07578	0.00181	1089	47
7.1	176	36	0.21	0.316	0.07430	0.00184	1050	49
8.1	43	6	0.14	1.020	0.07638	0.00859	1105	210
9.1	103	7	0.07	0.446	0.07513	0.00202	1072	53
10.1	96	24	0.25	0.707	0.07292	0.00249	1012	68
11.1	231	68	0.30	0.122	0.07534	0.00144	1077	38
12.1	38	14	0.37	0.188	0.07756	0.00336	1136	84
13.1	156	39	0.25	0.128	0.07504	0.00138	1070	37
14.1	226	26	0.12	0.162	0.07584	0.00120	1091	31
15.1	87	24	0.27	0.223	0.07510	0.00267	1071	70
6.2	158	29	0.18	0.063	0.07496	0.00168	1067	45
5.2	44	4	0.08	0.153	0.07840	0.00318	1157	78
9.2	90	9	0.10	0.125	0.07506	0.00353	1070	92
13.2	144	36	0.25	0.024	0.07513	0.00112	1072	30
16.1	219	75	0.34	0.154	0.07403	0.00122	1042	33
1.2	71	40	0.56	0.533	0.07584	0.00233	1091	60
17.1	89	14	0.16	0.114	0.07507	0.00249	1070	65
18.1	95	16	0.17	0.277	0.07593	0.00209	1070	65
19.1	102	25	0.25	2.844	0.07346	0.00544	1027	143
15.2	84	25	0.30	1.085	0.07312	0.00430	1017	115
15.3	122	40	0.33	0.456	0.07403	0.00206	1042	55

### 3. Paleomagnetism

#### Sampling and measurement

Paleomagnetic samples were collected from 25 sites in the western Bangemall Basin. Shale and mudstone host rocks were sampled in addition to dolerite at six sites, and shale samples only were collected at two sites. Sampling was conducted where structural control could be determined reliably by multiple measurements of bedding attitude in sedimentary rocks. Between 5 and 21 cores (typically 7 to 10), spread typically over several tens of metres, were drilled at each site and oriented using both magnetic and sun compasses. Measurements were conducted on 195 cores (332 specimens) from dolerite sills and 62 cores (62 specimens) from sedimentary rocks. Remanence composition was determined by detailed stepwise alternating field (AF) demagnetisation ( $\leq 26$  steps, up to 160 mT) of one specimen from each core, using the automated static method on the 2G-Enterprises cryogenic magnetometer described by Giddings et al. (1997). Duplicate specimens from about half of the collection were subjected to detailed stepwise thermal demagnetisation ( $\leq 20$  steps, 100 to  $>580^\circ\text{C}$ ), using a Magnetic Measurements thermal demagnetiser and 2G-Enterprises magnetometer. To monitor possible mineralogical changes during heating, magnetic susceptibility was measured in selected samples after each heating step using a Bartington MS2 susceptibility meter. Magnetic mineralogy was investigated from thermal demagnetisation characteristics and, in selected samples, from detailed variation of susceptibility versus temperature (20 to  $700^\circ\text{C}$ ) obtained using the Bartington meter in conjunction with an automated Bartington furnace. Magnetisation vectors were isolated using Principal Component Analysis (Kirschvink, 1980). Line segments were calculated with a minimum of four data points and a maximum angular deviation (MAD) of 10 to  $15^\circ$ .

#### Type L magnetisation

Two types of magnetic behaviour were observed: type **A** (described in main text) and type **L**. Type **L** magnetisations are characterised by high directional dispersion within individual sites, and by apparent unblocking temperatures and decreases in susceptibility between 200 and  $400^\circ\text{C}$ , mainly between 300 and  $350^\circ\text{C}$  (Figs. A1 and A2). **L** magnetisations are found in samples from 20 sites, and constitute the only remanence recognised at 9 sites. Both **A** and **L** magnetisations are found at 11 sites, in some cases together in the same samples. AF and thermal techniques yield similar directions. Variation in response to AF demagnetisation indicates the presence of both single-domain (SD) and multi-domain (MD) grains. The narrow temperature range over which intensities decrease, and its consistency in samples from over a wide area, suggests that the **L** magnetisation is a chemical remanent magnetisation (CRM) carried mainly by maghemite, rather than by MD magnetite or titanomagnetite, which are likely to show a greater range in unblocking temperature with slight differences in composition or grain size (Dunlop and Özdemir, 1997). The intensity and susceptibility decreases reflect inversion of maghemite to hematite during laboratory heating.

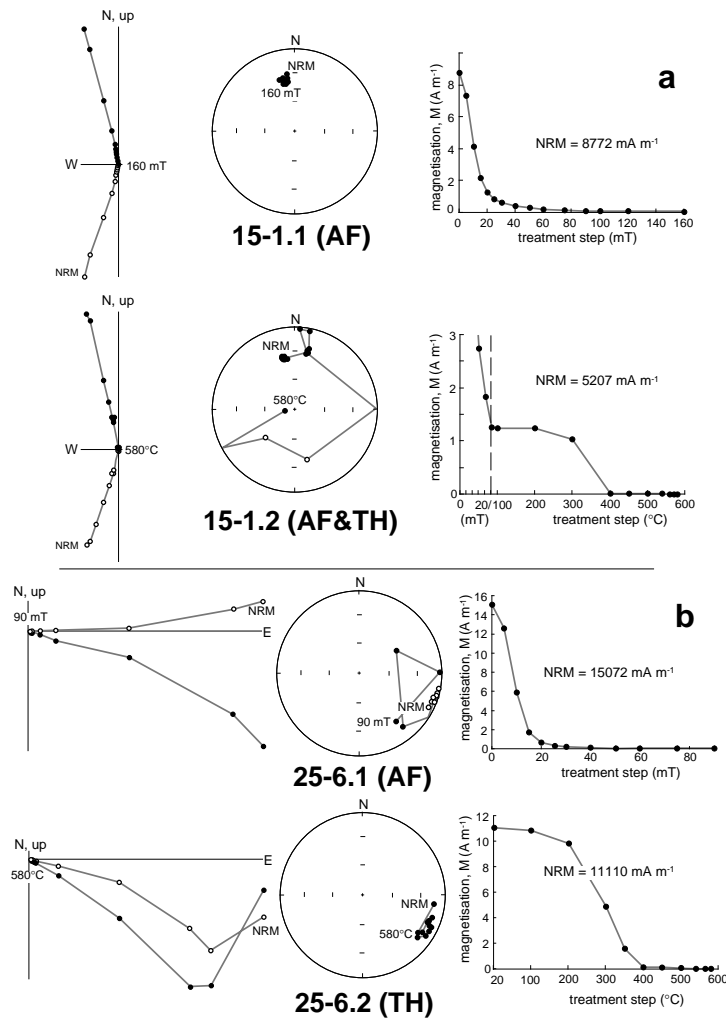


**Fig. A1.** Examples of AF and thermal demagnetisation of **L**-type remanence in two specimens of a single core from each of sites 15 (a) and 25 (b). Orthogonal projections show trajectories of vector endpoints during progressive demagnetisation (open/closed symbols represent vertical/horizontal plane). Open/closed symbols in lower-hemisphere equal-angle stereographic projections indicate upward/downward pointing directions. Reference frame is present horizontal. Demagnetisation curves show changes in magnetisation intensity during treatment.

The possibility that the **L** magnetisation is carried mainly by pyrrhotite, which has an unblocking temperature of 320°C and is relatively common in mafic intrusions, is unlikely. No evidence for pyrrhotite was observed in thermomagnetic (k-T) curves, and the presence of pyrrhotite does not explain the virtual absence of magnetic signatures attributable to magnetite (an essential mineral in fresh dolerite) in many **L**-type samples, an observation explained more readily by oxidation of primary magnetite to produce maghemite. Maghemite probably formed during weathering, burial within the basin, and/or fluid flow during deformation. Samples drilled within a few metres of each other yield similar directions in some cases, but those collected over tens of metres tend to give very different directions (Fig. A2). This outcrop-scale dispersion suggests that the **L** magnetisations are overprints acquired over an extended interval or at different times. Samples from two sills (sites 11 and 21) dated at 1465 Ma yielded only **L**-type magnetisations, and no coherent paleomagnetic direction could be determined for the older sill suite (e.g. Fig. A2b).

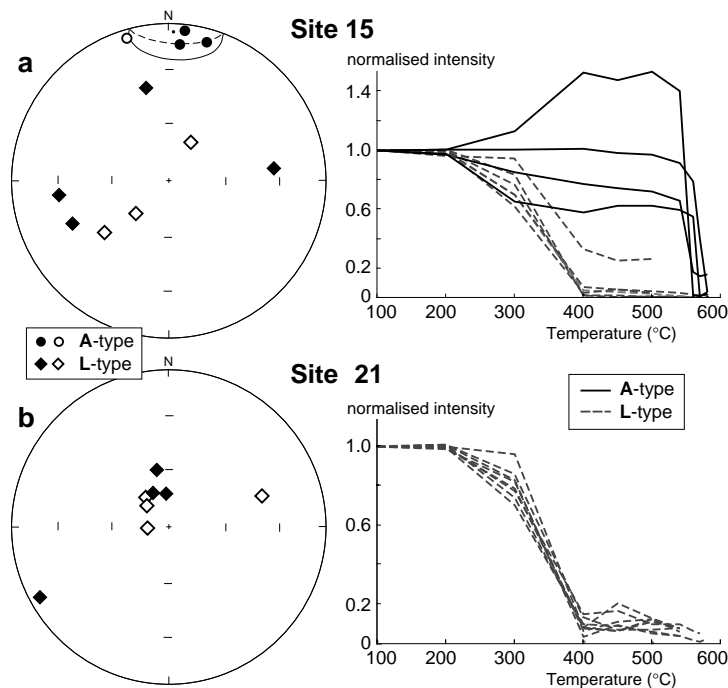


**Fig. A2.** Directions and thermal demagnetisation curves for **A**- and **L**-type magnetisations at site 15 (a) and **L**-type magnetisations at site 21 (b). Demagnetisation curves are normalised to values at 100°C. The mean direction and  $\alpha_{95}$  confidence circle are shown for four **A**-type directions at site 15. Other notes as in Fig. A1.

### Fold tests of **A**-component remanence

The cluster fold test of McFadden (1998) is positive, showing that within-group dispersion is consistent with between-group dispersion with the rocks unfolded, with the probability of exceeding the observed value of  $f = 1.27$  being 33%. The corresponding values for the rocks in their present folded state are  $f = 5.13$  and  $p = 0.6\%$ . The eigen analysis test of Tauxe and Watson (1994) shows that the tightest grouping of site-mean data is found between 72 and 113% unfolding (95% confidence limits). Both tests indicate that the **A** component magnetisation was acquired with the rocks in their unfolded position.

### Dyke baked-contact test

Paleomagnetic data have been obtained for a single NNE-trending dolerite dyke, located north of the study area, about 75 km from the nearest outcrops of Bangemall Supergroup. The primary nature of the dyke magnetisation is demonstrated by a positive baked-contact test with the 2.45 Ga Woongarra Rhyolite, into which the dyke is intruded (Fig. A3). The NE-up magnetisation in the host rhyolite may be primary or related to a widespread, late Paleoproterozoic low-temperature chemical and/or thermal overprint (Li et al., 1993; Schmidt and Clark, 1994). Paleomagnetic directions in the dyke and adjacent baked contact are similar to **A** component directions obtained in this study for 1070 Ma sills (Fig 4b). Two samples (#10, 11; Fig. A3) from the zone of partial remagnetisation exhibit both the regional country-rock direction and also directions intermediate between those of the dyke and unbaked host rock. Preservation of both dyke and host rock magnetisations indicates that no pervasive remagnetisation has occurred since the time of dyke intrusion. The dyke direction is similar to the **A** component observed in Bangemall sills, suggesting that the dyke and sills are similar in age, and supporting further the inference that the **A** magnetisation in the sills is original.

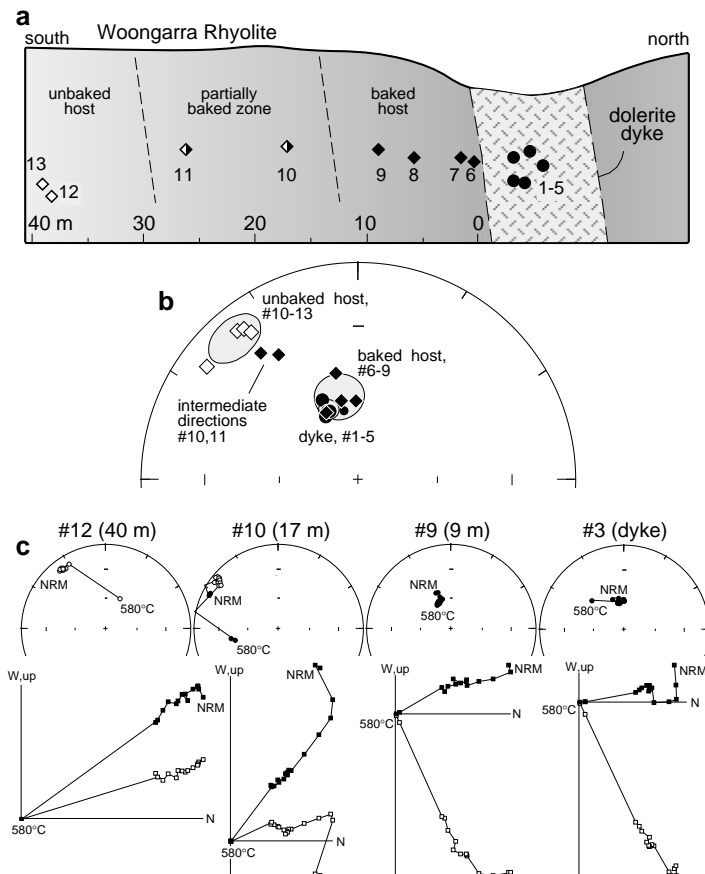


**Fig. A3.** (a) Outcrop sketch for the baked-contact test between a dolerite dyke and Woongarra Rhyolite. (b) Paleomagnetic directions;  $\alpha_{95}$  confidence circles are shown around the mean for each group. (c) Examples of thermal demagnetisation of four specimens (distance from the dyke contact shown in brackets). Other notes as in Fig. A1.

### Data from sills in the eastern Bangemall Basin

Paleomagnetic data have been obtained for 73 samples from nine sites in dolerite sills of the Glenayle area (Fig. 2a) in the eastern Bangemall Basin (M. Wingate, in prep.). Sills at six sites are flat-lying; three have bedding corrections of  $\leq 5^\circ$ . The mean direction is  $D, I = 346.3^\circ, +49.8^\circ$  ( $k = 64, \alpha_{95} = 6.5^\circ$ ), which is identical to those obtained in this study from the western Bangemall Basin (Figure 4b), indicating that the basin has undergone no internal vertical axis rotations since 1070 Ma.

### 4. Laurentian apparent polar wander (APW) path

Although the trend of the Laurentian APW path is well defined between  $\sim 1110$  and  $\sim 980$  Ma, age constraints for paleopoles younger than 1087 Ma are poor. The 1100 to  $\sim 1020$  Ma APW path in Figs. 1 and 5 is based on data from middle and upper Keweenawan rocks of the Lake Superior region that are well constrained stratigraphically and structurally (Table A4). The paleopoles were selected from a large data set (e.g. Halls and Pesonen, 1982; Weil et al., 1998) as the most reliable, having values of  $Q \geq 4$ , according to the paleomagnetic reliability scheme of Van der Voo (1990). Poles NSV, PLV, and LST are dated precisely by U-Pb on zircon (Davis and Paces, 1990; Davis and Green, 1997). The Nonesuch Shale (NS) conformably overlies the Copper Harbour Conglomerate (which contains the 1087 Ma Lake Shore Traps, LST), and in turn is overlain conformably by the Freda Sandstone (FS). The Freda Sandstone has a Rb-Sr whole-rock age of  $1046 \pm 46$  Ma (Chaudhury, in Henry et al., 1977),

contains native copper mineralisation dated by Rb-Sr on secondary minerals at 1040 – 1060 ( $\pm 20$ ) Ma (Bornhorst et al., 1988), and is cut by thrust faults inferred to have been active at 1060  $\pm$  20 Ma, based on Rb-Sr biotite cooling ages for uplifted basement rocks (Cannon et al., 1993). We have assigned an age of 1050  $\pm$  30 Ma to the mid-point between poles NS and FS. The Jacobsville Sandstone overlies the Freda Sandstone along an angular unconformity, and, at least in part, post-dates the 1060  $\pm$  20 Ma faulting (Cannon et al., 1993). We tentatively assign an age of 1020  $\pm$  30 Ma to this unit and its equivalent, the Chequamegon Sandstone. The APW path as defined here is not significantly different from that proposed by Ernst and Buchan (1993), or that of McElhinny and McFadden (2000, Table 7.4), which is based on four mean poles calculated from a large number of additional, less reliable data.

**Table A4** Selected late Mesoproterozoic paleopoles for Laurentia

Rock Unit	Pole	Lat (°N)	Long (°E)	<i>dp, dm</i> (°)	Q	Age constraints (Ma)	Paleomagnetic References
Abitibi dykes	AB	43	209	13,16	5	1141 $\pm$ 2 U-Pb baddeleyite	Ernst and Buchan, 1993
upper North Shore volcanics (mean)	NSV	32	184	4,6	5	1097 $\pm$ 2 U-Pb zircon	Halls and Pesonen, 1982
Portage Lake volcanics (mean)	PL	27	181	2,3	5	1095 $\pm$ 2 U-Pb zircon	Halls and Pesonen, 1982
Lake Shore Traps	LST	22	181	5,5	5	1087 $\pm$ 2 U-Pb zircon	Diehl and Haig, 1994
Nonesuch shale	NS	8	178	3,6	5	< 1087, ~1050 $\pm$ 30 Rb-Sr	Henry et al., 1977
Freda sandstone	FS	2	179	3,6	5	< NS, ~1050 $\pm$ 30 Rb-Sr	Henry et al., 1977
Jacobsville sandstone J(A+B)	JS	-9	183	3,6	4	< FS, > HA?, ~1020 $\pm$ 30	Roy and Robertson, 1978
Chequamegon sandstone	CS	-12	178	5,5	4	= JS, > HA?, ~1020 $\pm$ 30	McCabe and Van der Voo, 1983
Haliburton Intrusions A	HA	-36	143	10,11	4	980 $\pm$ 10 Ar-Ar	Buchan and Dunlop, 1976

Paleopoles labels refer to Fig. 5. Paleopoles are in present North American coordinates. *dp, dm* are the semi-axes of the oval of 95% confidence about the paleopole. Q is the paleomagnetic reliability index of Van der Voo (1990). References for ages are provided in the text.

## References

- Bornhorst, T.J., Paces, J.B., Grant, N.K., Obradovich, J.D. and King Huber, N., 1988. Age of native copper mineralisation, Keweenaw Peninsula, Michigan. *Econ. Geol.*, **83**, 619-625.
- Buchan, K.L. and Dunlop, D.J., 1976. Paleomagnetism of the Haliburton Intrusions: superimposed magnetisations, metamorphism, and tectonics in the late Precambrian. *J. Geophys. Res.*, **81**, 2951-2966.
- Cannon, W.F., Peterman, Z.E. and Sims, P.K., 1993. Crustal-scale thrusting and origin of the Montreal River Monocline – a 35-km thick cross section of the Midcontinent Rift in northern Michigan and Wisconsin. *Tectonics*, **12**, 728-744.
- Compston, W., Williams, I.S. and Meyer, C., 1984. U-Pb geochronology of zircons from lunar breccia 73217 using a sensitive high mass-resolution ion microprobe. *J. Geophys. Res.*, **89**, B525-B534.
- Cumming, G.L. and Richards, J.R., 1975, Ore lead isotope ratios in a continuously changing Earth. *Earth Planet. Sci. Lett.*, **28**, 155-171.
- Davis, D.W. and Green, J.C., 1997. Geochronology of the North American Midcontinent Rift in western Lake Superior and implications for its geodynamic evolution. *Can. J. Earth Sci.*, **34**, 476-488.
- Davis, D.W. and Paces, J.B., 1990. Time resolution of geologic events on the Keweenaw Peninsula and implications for development of the Midcontinent Rift system. *Earth Planet. Sci. Lett.*, **97**, 54-64.
- Diehl, J.F and Haig, T.D., 1994. A paleomagnetic study of the lava flows within the Copper Harbour Conglomerate, Michigan: new results and implications. *Can. J. Earth Sci.*, **31**, 369-380.
- Dunlop, D.J. and Özdemir, Ö, 1997. *Rock Magnetism: fundamentals and frontiers*. Cambridge University Press, 573 p.
- Ernst, R.E. and Buchan, K.L., 1993. Paleomagnetism of the Abitibi dike swarm, southern Superior Province, and implications for the Logan Loop. *Can. J. Earth Sci.*, **30**, 1886-1897.
- Giddings, J.W., Klootwijk, C.T., Rees, J. and Groenewoud, A., 1997. Automated AF-demagnetisation on the 2-G Enterprises through-bore, cryogenic magnetometer. *Geologie en Mijnbouw*, **76**, 35-44.
- Halls, H.C. and Pesonen, L.J., 1982. Paleomagnetism of Keweenawan rocks. *Geol. Soc. Am., Mem.* **156**, 173-201.
- Henry, S.G., Mauk, F.J., and Van der Voo, R., 1977. Paleomagnetism of the upper Keweenawan sediments: the Nonesuch Shale and Freda Sandstone. *Can. J. Earth Sci.*, **14**, 1128-1138.
- Kirschvink, J.L., 1980. The least-squares line and plane and the analysis of paleomagnetic data. *Geophys. J. R. Astr. Soc.*, **62**, 699-718.
- Li, Z.-X., Powell, C.McA. and Bowman, R., 1993. Timing and genesis of Hamersley iron-ore deposits. *Expl. Geophys.*, **24**, 631-636.

- McCabe, C. and Van der Voo, R., 1983. Paleomagnetic results from the upper Keweenaw Chequamegon Sandstone: implications for red bed diagenesis and Late Precambrian apparent polar wander of North America. *Can. J. Earth Sci.*, **20**, 105-112.
- McElhinny, M.W. and McFadden, P.L., 2000. *Paleomagnetism – Continents and Oceans*. International Geophysics Series Vol. 73, Academic Press, USA.
- McFadden, P., 1998. The fold test as an analytical tool. *Geophys. J. Int.*, **135**, 329-338.
- McLaren, A.C., Fitzgerald, J.D., and Williams, I.S., 1994. The microstructure of zircon and its influence on the age determination from Pb/U isotopic ratios measured by ion microprobe. *Geochim. Cosmochim. Acta*, **58**, 993-1005.
- Nelson, D.R., 1997. Compilation of SHRIMP U-Pb zircon geochronological data, 1996. *W. Aust. Geol. Surv. Rec. 1997/2*, 189p.
- Roy, J.L. and Robertson, W.A., 1978. Paleomagnetism of the Jacobsville Formation and the apparent polar path for the interval ~1100 to ~670 m.y. for North America. *J. Geophys. Res.*, **83**, 1289-1304.
- Schmidt, P.W. and Clark, D.A., 1994. Palaeomagnetism and magnetic anisotropy of Proterozoic banded-iron formations and iron ores of the Hamersley Basin, Western Australia. *Precamb. Res.*, **69**, 133-155.
- Steiger, R.H. and Jäger, E., 1977. Subcommittee on geochronology: convention on the use of decay constants in geo- and cosmochronology. *Earth Planet. Sci. Lett.*, **36**, 359-362.
- Tauxe, L. and Watson, G.S., 1994. The fold test: an eigen analysis approach. *Earth Planet. Sci. Lett.*, **122**, 331-341.
- Van der Voo, R., 1990. The reliability of paleomagnetic data. *Tectonophys.*, **184**, 1-9.
- Weil, A.B., Van der Voo, R., Mac Niocall, C. and Meert, J.G., 1998. The Proterozoic supercontinent Rodinia: paleomagnetically derived reconstructions for 1100 to 800 Ma. *Earth Planet. Sci. Lett.*, **154**, 13-24.
- Wingate, M.T.D. and Compston, W., 2000. Crystal orientation effects during ion microprobe U-Pb analysis of baddeleyite. *Chem. Geol.*, **168**, 75-97.